Acta Crystallographica Section B
Structural Science
ISSN 0108-7681

Crystal structure of the inclusion complex of β-cyclodextrin with mefenamic acid from high-resolution synchrotron powder-diffraction data in combination with molecular-mechanics calculations

Mihaela M. Pop,[a]* Kees Goubitz,[a] Gheorghe Borodi,[b] Mircea Bogdan,[b] Dirk J. A. De Ridder,[a] Rene Peschar[a] and Henk Schenk[a]

[a]University of Amsterdam, Faculty of Science, Laboratory for Crystallography, Institute of Molecular Chemistry, Nieuwe Achtergracht 166, NL-1018 WV Amsterdam, The Netherlands, and [b]National Institute for Research and Development of Isotopic and Molecular Technologies, PO Box 700, R-3400 Cluj-Napoca, Romania

Correspondence e-mail: mihaela@science.uva.nl

Received 2 October 2002
Accepted 22 October 2002

The crystal structure of the inclusion complex of β-cyclodextrin with mefenamic acid has been determined from a combination of high-resolution synchrotron powder-diffraction data and molecular-mechanics calculations. A grid search indicates two possible solutions, which are corroborated by molecular-mechanics calculations, while Rietveld-refinement results suggest the crystal structure that is more likely to be formed in the solid state. Mefenamic acid is partially included in β-cyclodextrin with either the xylyl or the benzoic-acid moiety being inside its cavity. In both solutions mefenamic acid and β-cyclodextrin form a monomeric complex in a herringbone packing scheme.

1. Introduction

Cyclodextrin (CD) molecules are macrocyclic oligosaccharides that consist of glucose units that are α-1,4-glycosidically linked in a cyclic fashion. α-, β- and γ-CDs are the three most commonly used CDs in inclusion-complex research and consist of six, seven (Fig. 1*a*) and eight glucose units, respectively. In general, CDs are characterized by a 'hollow' truncated conical shape; the primary face (with the smaller radius) of the truncated cone comprises the primary hydroxyl groups of the glucose units and the secondary face comprises (twice as many) secondary hydroxyl groups. CDs consist of a hydrophobic cavity relative to a hydrophilic periphery of the molecule. Consequently, CDs are soluble in aqueous media and are able to encapsulate hydrophobic guest molecules within their cavities and form CD inclusion complexes. In α-, β- and γ-CDs the O4 atoms that link the glucose units, and thus form the so-called CD-O4(G_n) glycosidic plane, are nearly coplanar and form almost regular polygons. The overall shape of the CD macrocycle in inclusion complexes can be regular or distorted; the shape depends on the guest molecule and the crystal environment.

The production of inclusion compounds by pharmaceutical and chemical industries has increased considerably in recent years (Fromming & Szejtli, 1994) because of the role of CDs as solubilizers, stabilizers and carriers of poorly soluble drug molecules (D'Souza & Lipkowitz, 1998; Irie & Uekama, 1997; Loftsson & Brewster, 1996; Rajewski & Stella, 1996).

Mefenamic acid {2-[(2,3-dimethylphenyl)amino]benzoic acid, MF; Fig. 1(*b*)} is a non-steroid drug that is commonly used in therapeutics because of its strong analgesic, antipyretic and anti-inflammatory properties (Kostkowski & Kubikowski, 1994; Nogrady, 1988). Unfortunately, the very low aqueous solubility of MF (6.1 μg ml^{-1} at pH = 5.6) causes undesirable side effects such as nausea, rash and vomiting when adminis-

tered orally. These side effects can be reduced by increasing the drug solubility, which enhances its bioavailability and may permit a lower dose.

A successful method used to increase not only the water solubility but also the stability of the drug is the complexation with CDs (Ammar *et al.*, 1997; Palmieri *et al.*, 1997; Loftsson, Baldvinsdottir & Sigurdardottir, 1993; Loftsson, Olafsdottir *et al.*, 1993; Loftsson & Petersen, 1997). In order to understand the biopharmaceutical functions of the drug molecules we need to investigate the forces driving the complexation and the structure of inclusion complexes.

The β-CD/MF inclusion complex was obtained recently by coprecipitation from diethyl ether. The effect of the β-CD on the solubility and stability of MF was analysed (Hladon *et al.*, 1999), but no crystal structure of this complex has been determined so far. The stability constants of the complex, which were determined by potentiometric methods, revealed non-stoichiometric molar ratios of host-to-guest molecules, which are highly dependent on the precipitation conditions of the complex. The logarithmic values of these stability constants showed that MF forms a weak inclusion complex, but the solubility and stability increases when it is complexed with β-CD.

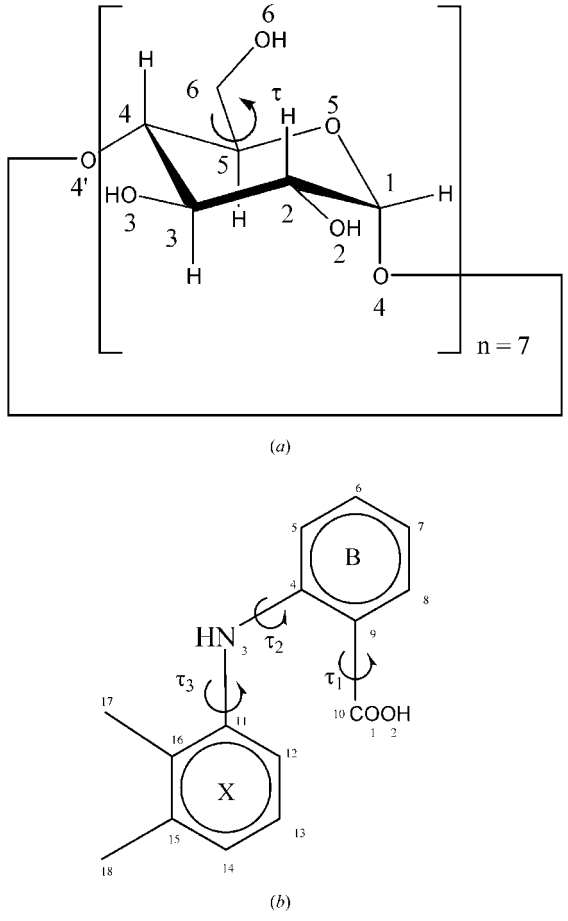

Figure 1
(*a*) Schematic diagram of β-CD. (*b*) Chemical diagram of mefenamic acid; the varied torsion angles are indicated (*X* and *B* are the xylyl moiety and benzoic acid moiety, respectively).

X-ray powder diffraction has been used for the identification of CD complexes and their qualitative characterization by the comparison of the powder patterns of the host, the guest and the host–guest mixture. These patterns can indicate inclusion-complex formation (Atwood *et al.*, 1996; Hladon *et al.*, 1999). Because the crystal-packing arrangement of the inclusion complex is generally quite different from that of the individual components, a new inclusion species is usually characterized by its specific 'fingerprint'. In order to extend the use of X-ray powder diffraction for the analysis of CD inclusion complexes with organic guests, Caira (2003) has recently attempted to show that the majority of these complexes crystallize in a few distinct isostructural classes and that the powder patterns for a given class are essentially the same, regardless of the nature of the included guest. A series of reference powder patterns were derived from the available single-crystal data, and these patterns allowed the identification of new CD inclusion complexes without any quantitative structural characterization.

In this paper we report the crystal structure of the β-CD/MF inclusion complex as solved with powder-based grid-search techniques (Chernyshev & Schenk, 1998) that use two starting models that were obtained by molecular mechanics in *Cerius* (Molecular Simulation Inc., 1995). To our knowledge this is the first crystal-structure determination of a β-CD inclusion complex from powder-diffraction data. We demonstrate that this type of data can provide a more detailed structural characterization of CD inclusion complexes than is possible with just a qualitative identification.

2. Experimental

2.1. Synthesis

β-CD was purchased from Sigma Chemie GmbH (Germany). The compound contained, on average, eight water molecules. MF was converted to an MF—Na salt (pH = 12) by titration with 0.1 N NaOH; 10 m*M* aqueous solutions of the MF—Na salt and β-CD were prepared. Equal amounts (25 ml) of β-CD and MF—Na salt were mixed, shaken for 8 h and then stored for 7 d at 313 K. The precipitate of the inclusion complex was washed twice with small portions of distilled water and was dried first in air and then in a dryer at 325 K. β-CD was used without further purification and the water content was considered in the calculation of the solute concentration. Elemental analysis of the inclusion complex was not performed but it is very probable that the inclusion complex still contains water.

2.2. High-resolution synchrotron powder-diffraction measurements

A capillary of diameter 0.7 mm was filled with powder and measured at the high-resolution powder station of BM16 (Fitch, 1996) at the European Synchrotron Radiation Facility (Grenoble, France) with $\lambda = 0.80081$ Å. The capillary was rotated during exposure. Continuous scans were made from 0.0° to 48.0° in 2θ, with 0.5° 2θ min^{-1} and a sampling time of

50 ms. We did not measure every 2θ range for the same amount of time; rather, the higher-angle regions of the patterns were measured several times in order to mimic a single-crystal measurement, *i.e.* to give every reflection the same data-collection time. After data collection the scans were binned in 0.005° intervals of 2θ and scaled.

The peaks were located using the program *PROFIT* 1.0*c* (Philips Electronics NV, 1996), and the cell and space group were found with *ITO* (Visser, 1969) (see Table 1 for crystallographic data).[1]

3. Modelling strategy, structure solution and refinement

3.1. Model building

The initial model of the β-CD inclusion complex with MF was constructed from single-crystal structures that were found in the Cambridge Structural Database (CSD; Allen & Kennard, 1993); the β-CD model was taken from the CSD entry with refcode BCDEXD03 (Steiner & Koellner, 1994) and the MF model from XYANAC (McConnell & Company, 1976). BCDEXD03 was chosen because it crystallizes in $P2_1$, it has no inclusion compound and it has $R \leq 0.07$. Since BCDEXD03 has two disordered primary hydroxy groups, only the O atom that points outwards was taken into account. In the initial search models, H atoms were considered for MF but not for β-CD. Because of the observed non-stoichiometry of the host–guest molar ratio and the frequently observed disorder in β-CD inclusion complexes (for example, Steiner & Koellner, 1994; Makedonopoulou & Mavridis, 2000), it was assumed that the positioning of an approximate model by means of a grid-search technique based on powder data alone could prove difficult. Therefore, in order to get a more probable molecular geometry of both the host and guest fragments, molecular-mechanics simulations were performed in *Cerius* (Molecular Simulation Inc., 1995). For this purpose, both fragments were positioned in the unit cell that resulted from the indexing of the experimental powder pattern of the inclusion complex in space group $P2_1$. In the initial models that were used in the molecular-mechanics simulations, MF was fully encapsulated in the β-CD fragment with either the xylyl or the benzoic acid moieties situated at the β-CD primary face. With these initial models an energy-minimization procedure was carried out, which used fixed unit-cell parameters as constraints and rigid-body descriptions of the MF phenyl moieties and the β-CD molecule. For the definition of the potential energy in *Cerius* (Molecular Simulation Inc., 1995) the consistent valence force-field was used, which can handle a wide range of organic systems.

After energy minimization the two models (to be referred to as I and II) were found to be almost isoenergetic (energy difference of $\sim$84 kJ mol^{-1}) and MF had become only partially encapsulated in the CD macrocycle. Either the xylyl (I) or the benzoic acid (II) moiety was inside the cavity, and the N atom that linked the two phenyl rings was found at the secondary face of the macrocycle in both cases, thus the remainder of the MF was left outside the cavity. In the two energy-minimized models the MF ring inside the β-CD cavity makes approximately the same angle with the CD—O4(G_n) plane [67° for (I) and 62° for (II)] while the outer MF ring bends more towards the O4(G_n) plane of the macrocycle [dihedral angles between the outer MF ring and the O4(G_n) plane are 36° for (I) and 48° for (II)]; G denotes a glucose unit. The orientation of the MF rings relative to each other seems to be stabilized by an intramolecular hydrogen bond between the N atom and one O atom of the benzoic acid moiety

Table 1
Experimental details.

The second line for 2θ range, goodness of fit (GoF), R_p and R_{wp} indicates the results of the full-pattern decomposition procedure.

	(I)	(II)
Crystal data		
Chemical formula	$C_{55.5}H_{13.5}N_{0.9}O_{36.8}$	$C_{55.5}H_{13.5}N_{0.9}O_{36.8}$
Chemical formula weight	1281.59	1281.59
Cell setting, space group	Monoclinic, $P2_1$	Monoclinic, $P2_1$
a, b, c (Å)	15.4797 (9), 25.5892 (15), 9.2973 (5)	15.4797 (5), 25.5892 (10), 9.2973 (4)
β (°)	98.976 (7)	98.976 (3)
V (Å^3)	3637.7 (4)	3637.7 (2)
Z	2	2
D_x (Mg m^{-3})	1.17	1.17
Radiation type	Synchrotron	Synchrotron
2θ range (°)	3.205–39.995 3.2–40.0	3.205–39.995 3.2–40.0
Temperature (K)	295	295
Data collection		
Diffractometer	ESRF BM16	ESRF BM16
No. of measured datapoints	7359	7359
No. of reflections	2446	2446
Refinement		
No. of bond restraints	72	72
No. of angle restraints	51	51
No. of planar restraints	3	3
No. of rigid bodies	7	7
No. of variables		
Structural		
Lattice	4	4
Positional	141	141
Thermal	2	2
Other		
Texture	63 (L = 14)	63 (L = 14)
Profile	9	9
Background	10	10
GoF	6.08 3.19	7.08 3.19
R_p† (%)	9.80 5.26	11.16 5.26
R_{wp}‡ (%)	13.32 7.06	15.67 7.06

† $R_p = \sum |y_{obs} - y_{calc}| / \sum y_{obs}$. ‡ $R_{wp} = \left[\sum w(y_{obs} - y_{calc})^2 / \sum w y_{obs}^2\right]^{1/2}$.

[1] Supplementary data for this paper are available from the IUCr electronic archives (Reference: NA0142). Services for accessing these data are described at the back of the journal.

Table 2
Characteristics of β-CD.

D = distances between atoms O4(G_n)···O4(G_{n+1}); φ = angles between atoms O4(G_{n-1})···O4(G_n)···O4(G_{n+1}); d = deviations from the least-squares plane through the seven O4(G_n) atoms; α = dihedral angle between the O4(G_n) plane and the least-squares plane through C2(G_n), C3(G_n), C5(G_n) and O5(G_n); $D3$ = intramolecular distances between atoms O2(G_n)···O3(G_{n+1}). Torsion angles τ_a = O5(G_n)—C5(G_n)—C6(G_n)—O6(G_n), τ_b = C4(G_n)—C5(G_n)—C6(G_n)—O6(G_n).

Residue	Solution	D (Å)	φ (°)	d (Å)	α (°)	$D3$ (Å)	τ_a (°)	τ_b (°)
G1	I	5.25 (4)	132.2 (9)	0.04 (3)	69.6 (10)	4.69 (4)	97 (3)	−151 (3)
	II	5.31 (4)	128.3 (9)	−0.06 (4)	69.6 (10)	5.24 (4)	−80 (5)	37 (7)
G2	I	4.14 (4)	119.1 (9)	0.09 (4)	59.8 (11)	2.91 (3)	102 (4)	−133 (3)
	II	4.61 (5)	131.1 (9)	0.04 (5)	53.9 (11)	2.91 (4)	157 (4)	−89 (5)
G3	I	5.28 (4)	137.7 (9)	0.18 (4)	75.8 (8)	4.16 (2)	172 (3)	−73 (3)
	II	4.53 (4)	137.0 (8)	0.17 (5)	64.8 (9)	4.19 (3)	60 (3)	172 (3)
G4	I	4.80 (4)	120.3 (8)	−0.38 (4)	73.1 (9)	3.63 (2)	135 (4)	−110 (4)
	II	4.96 (4)	115.3 (8)	−0.17 (4)	71.2 (10)	3.19 (3)	165 (4)	−82 (4)
G5	I	5.19 (4)	120.8 (8)	0.46 (4)	57.2 (8)	4.31 (3)	47 (6)	−169 (4)
	II	4.87 (4)	129.2 (9)	0.13 (4)	46.9 (12)	4.55 (4)	76 (3)	−158 (2)
G6	I	4.94 (4)	122.7 (7)	−0.16 (4)	78.9 (9)	3.24 (3)	−96 (3)	33 (4)
	II	4.70 (4)	145.8 (8)	−0.03 (4)	55.0 (10)	3.34 (3)	−34 (6)	−178 (4)
G7	I	3.11 (3)	141.5 (8)	0.01 (3)	70.9 (10)	2.15 (4)	−103 (3)	105 (3)
	II	4.80 (4)	112.2 (6)	0.00 (3)	70.3 (11)	2.46 (3)	−118 (5)	122 (4)

[N3···O1 = 2.8 Å and 2.9 Å; N3—H19···O1 = 130° and 127° for (I) and (II), respectively].

3.2. Structure determination and refinement

To obtain reflection intensities a full-pattern decomposition (FPD) procedure was performed with the program *MRIA* (Zlokazov & Chernyshev, 1992). The high-resolution synchrotron powder-diffraction pattern was fitted employing a split-type pseudo-Voigt peak-profile function (Toraya, 1986). Some details of the FPD procedure are listed in Table 1.

To position the molecules in the asymmetric part of the unit cell, the models that were obtained after energy minimization were used in an in-house modified version of the grid-search procedure (Chernyshev & Schenk, 1998) that is implemented in the program *MRIA* (Zlokazov & Chernyshev, 1992). We used 200 low-angle X_{obs} values that were extracted from the patterns after the FPD procedure. Because both models were calculated to have almost the same energies, both models were taken into account in the grid-search procedure. Instead of the original grid search, the position and orientation of the starting models for CD and MF were optimized using a genetic algorithm with $R(X)$ as the cost function [X_{obs} and $R(X)$ are defined in expressions (1) and (2) of Chernyshev & Schenk (1998)]. In order to get better starting models for the Rietveld refinement (RR), both fragments were treated as independent; for MF three torsion angles were varied (Fig. 1*b*, Table 2) while for CD rotation around the C5—C6 bond of all primary hydroxy groups (Fig. 2) was allowed. For each of the starting models this procedure led to a possible solution with a minimum around $R(X) = 64\%$. The two solutions have a different part of MF entering the secondary face of β-CD: the xylyl moiety (I) or the benzoic acid moiety (II).

RR was performed with *GSAS* (Larson & Von Dreele, 1994). The multi-term Simpson's rule integration of the pseudo-Voigt profile function (Howard, 1982) was used and its first nine coefficients were refined. The preferred orientation was corrected using the spherical-harmonics function that is implemented in *GSAS* (Von Dreele, 1997). A cylindrical sample symmetry was chosen and a maximum harmonic order $L = 14$ was considered.

In order to retain a chemically realistic model each glucose unit together with its secondary O atoms was defined as a separate rigid body and rotation and translation were allowed relative to the glycosidic plane. In addition, planar restraints were applied to the seven O4(G_n) atoms and to the MF phenyl moieties. Since the primary units of the host molecule are more flexible they were not included in the rigid-bodies definition. Bond-distance and bond-angle restraints were applied to the primary OH groups (C5—C6—O6), the glycosidic O4(G_n) atoms and MF. The weight factors (f_d, f_a, f_p), which weight the effect of distance, angle and planar restraints on the minimization function, were gradually reduced in subsequent refinement cycles (f_d from 10000 to 500; f_a from 1000 to 10; f_p from 10000 to 1000). U_{iso} values of identical atom types were coupled during the refinement. In the final refinement cycles a better fit was obtained by using an occupancy factor of 0.9 for MF (see §1). After RR, convergence was obtained for both solutions with $R_{wp} = 13.3\%$, $R_p = 9.8\%$ for (I) and $R_{wp} = 15.7\%$, $R_p = 11.2\%$ for (II).

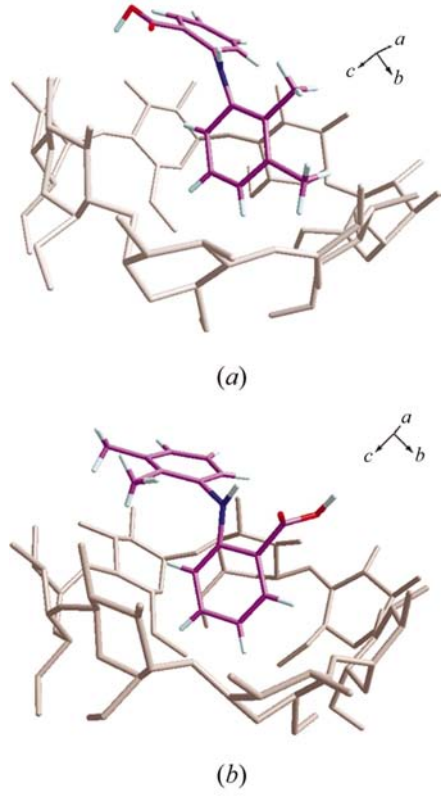

Figure 2
(*a*) CD/MF solution (I). (*b*) CD/MF solution (II).

The relevant crystal data and RR results are presented in Table 1. Plots of observed and calculated X-ray diffraction patterns, a difference plot after RR and a *DIAMOND* plot (Pennington, 1999) of the compounds are depicted in Figs. 2 and 3.

4. Results and discussion

Taking into account the existence of bimodal inclusion complexes in CD compounds, as evidenced by NMR experiments combined with molecular-mechanics calculations (Fronza *et al.*, 1992; Fathallah *et al.*, 1994; Salvatierra *et al.*, 1996), both of the solutions obtained by RR could well be present. On the other hand, the significantly better fit obtained for (I) (Fig. 3*a*) suggests that in the solid state the solution that has the xylyl moiety partially included in the CD cavity is more likely to be formed than solution (II), which has the benzoic acid moiety included in the CD cavity (Fig. 3*b*).

4.1. Geometries of the guest molecules after RR

The characteristics of the β-CD moiety are presented in Table 2. α is the dihedral angle between the O4(G_n) plane and the least-squares plane through the C2, C3, C5 and O5 atoms of each G_n glucose unit; $\alpha = 90^\circ$ means that the plane through these four glucose atoms is perpendicular to the O4(G_n) macrocycle plane and thus indicates that the glucose unit is not tilted.

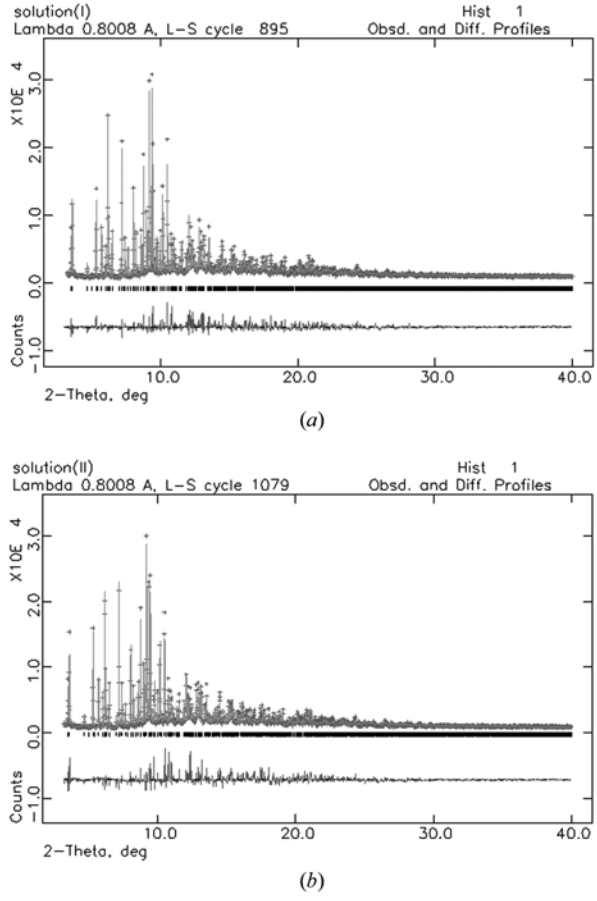

Figure 3
(*a*) Calculated (−) and observed (+) powder pattern after the final Rietveld refinement of solution (I). (*b*) Calculated (−) and observed (+) powder pattern after the final Rietveld refinement of solution (II). Markers of all reflections are included.

The seven glycosidic O4(G_n) atoms form a distorted heptagon. The O4(G_n) interatomic distances and angles differ significantly from the ideal values in a non-distorted heptagon (4.38 Å and 128.6°; Mentzafos *et al.*, 1991) and the differences are larger than those usually observed in β-CD inclusion compounds (for example, Steiner & Koellner, 1994; Makedonopoulou & Mavridis, 2000).

In (I), the distorted heptagon is characterized by side lengths in the range 4.14–5.28 Å for G1—G6 residues and angles in the range 119.1–141.5° for all glucose units. O4(G7)—O4(G1) differs significantly from O4(G1)—O4(G2); this difference can be attributed to the steric effects from the MF xylyl moiety, which is in van der Waals contact with glucose residues G1 and G2. The distorted conformation of the β-CD cavity is also reflected by the deviations from planarity of O4(G4) and O4(G5) relative to the O4(G_n) glycosidic plane, the deviations of the other O4(G_n) atoms being relatively small (Table 2). On the other hand, the large tilt angles $|90^\circ - \alpha|$ of the glucose units towards the pseudo-sevenfold axis of the O4(G_n) mean plane compared with the mean values encountered in CD complexes (|90°–84°|) (Makedonopoulou *et al.*, 1999) indicate the narrowing of the β-CD primary face. Consequently, only two possible intramolecular hydrogen bonds exist between the secondary hydroxyl O atoms of the glucose residues: O2(G7)···O3(G1) = 2.15 (4) Å and O2(G2)···O3(G3) = 2.91 (3) Å (Table 2). The other O2(G_n)···O3(G_{n+1}) distances are between 3.24 and 4.69 Å and cause an enlargement of the secondary face of β-CD.

The seven glucose units show distorted chair conformations. The torsion angles τ_a about the exocyclic C5—C6 bonds of the C5—C6—O6 primary groups correspond to an anticlinal (+*ac*) orientation for the G1 and G2 primary groups, while the G5 primary unit adopts a *gauche* (+*sc*) orientation (Moss, 1996), which points into the macrocycle cavity and closes up the opposite sides of the CD primary face. The guest inclusion towards the primary CD face is therefore blocked. The other primary CD groups have an anticlinal orientation (+*ac* for G4, −*ac* for G6 and G7), while the G3 primary unit adopts a *trans* (+*ap*) orientation (τ_a; Table 2).

In (II) the CD macrocycle distortions are less severe (Table 2). The tilting of glucoses towards the CD cavity, however, is significantly larger and the orientations of the primary glucose units are different from those in (I) [see τ_a in Table 2: *gauche* for G1 (−*sc*), G3 (+*sc*), G5 (+*sc*), G6 (−*sc*); +*ap* for G2, G4 and −*ac* for G7].

The distortions of the CD macrocycle in the inclusion complex could be caused by MF. Another possible explanation is that, for most of the RR, water molecules were not considered in the models because of the lack of stoichiometric information. After convergence the calculated solvent-accessible areas for (I) (Spek, 1990) allow for the presence of one water molecule inside the CD cavity and of five more in the

Table 3
Intramolecular (*) and intermolecular hydrogen bonds between MF and β-CD.

D—H	A	H···A (Å)	D···A (Å)	D—H···A (°)
(I)				
N3—H19*	O1	2.39	2.84 (5)	108
C17—H28	O6(G5)^{i}	1.58	2.50 (4)	155
C17—H27	O5(G4)^{i}	2.28	3.31 (2)	159
C18—H24	O4(G1)	2.17	2.83 (3)	123
C18—H23	O2(G1)	2.42	3.13 (3)	126
C18—H25	O5(G1)	2.44	3.35 (3)	150
C5—H29	O3(G6)	1.74	2.45 (2)	128
N3—H19	O5(G4)^{i}	1.64	2.59 (4)	167
C7—H31	O2(G7)^{ii}	2.44	3.18 (3)	134
(II)				
N3—H19*	O1	2.23	2.80 (5)	114
C6—H30	O6(G5)	1.99	2.67 (3)	123
O2—H33	O6(G5)^{i}	2.01	2.41 (4)	102
C14—H22	O2(G7)^{ii}	2.47	3.38 (3)	151
C18—H24	O3(G5)	2.47	3.32 (2)	143
N3—H19	O5(G4)^{i}	1.88	2.83 (4)	157

Symmetry codes: (i) $x, y, -1+z$; (ii) $1-x, -\frac{1}{2}+y, -z$.

space between the CD molecules, while for (II) there is only space for about nine water molecules outside the CD cavity. Attempts to include water in the RR were not successful. This is not surprising because it is well known that water molecules can be orientationally disordered and alternatively form hydrogen bonds with different neighbours (Steiner & Koellner, 1994; Betzel *et al.*, 1984).

4.2. Guest conformation, mode of inclusion and crystal packing

For both solutions, the 0.9 occupancy factor for MF is in agreement with the observed non-stoichiometric ratio of the host-to-guest molecules in β-CD/MF inclusion complexes (Hladon *et al.*, 1999).

MF is partially included in the CD macrocycle and enters by the secondary face of the macrocycle. Similar cases where the CD cavity is partially occupied by the inclusion compound have been reported (Caira *et al.*, 1994; Rontoyianni *et al.*, 1998; Makedonopoulou *et al.*, 2001).

In both (I) and (II) one of the phenyl moieties is located outside the CD cavity, and the N atom that links the two phenyl rings is situated at the secondary face of the CD macrocycle with a hydrogen bond to the G4 glucose unit of a neighbouring CD molecule (Table 3).

The MF intramolecular hydrogen bond N3—H19···O1 that is present in the energy-minimized model is maintained. Compared with the model after energy minimization, the orientation of the two phenyl rings has changed both relative to each other and relative to the O4(G_n) plane. The differences in the MF torsion angles after energy minimization, after grid search and after RR are presented in Table 4. The included moiety [xylyl for (I) and benzoic acid for (II)] enters almost perpendicularly into the host cavity: the dihedral angles between the included planar moieties and the O4(G_n) plane are 80.5 (6)° for (I) and 76.7 (14)° for (II). The outside phenyl ring is in both cases bent towards the secondary face of

Table 4
Torsion angles varied in the grid-search (GS) procedure.

Comparison with the values that resulted after energy minimization (EM) and Rietveld refinement (RR).

Torsion angle	(I) after EM	(I) after GS	(I) after RR	(II) after EM	(II) after GS	(II) after RR
C4—C9—C10—O2	−158	−158	−172 (3)	−158	−71	−127 (5)
C11—N3—C4—C5	−80	−64	−47 (9)	−40	−29	−13 (9)
C4—N3—C11—C12	−75	−62	−58 (7)	−58	−86	−101 (4)

the macrocycle: the dihedral angles between the outside planar moieties and the O4(G_n) plane are 13.1 (7)° for (I) and 9.0 (12)° for (II). The dihedral angles between the MF phenyl rings are 85.5 (10)° and 70.8 (18)° for (I) and (II), respectively.

In (I) one of the methyl groups of the xylyl moiety is situated outside the CD macrocycle and is hydrogen bonded to both the primary O6(G5) atom and the glycosidic O5(G4) atom of the neighbouring β-CD in the direction of the *c* axis. The other methyl group is inside the host cavity and forms three intermolecular hydrogen bonds with O atoms of G1 of its CD host molecule (Table 3). Probably all eight of the intermolecular hydrogen bonds that involve the MF acid, its CD host and two neighbouring CD molecules hold the included phenyl ring at the secondary face of CD.

In (II) both O atoms of the included benzoic moiety are situated outside the host cavity. The primary O6(G5) atoms of two neighbouring CD molecules form hydrogen bonds with the guest benzoic ring and with its outer O2 atom. Besides these interactions, there are two more hydrogen bonds between the outer phenyl ring and neighbouring CD molecules (Table 3).

Instead of a dimeric β-CD complex formation, which is usually favoured in β-CDs complexed with relatively large guests (Mentzafos *et al.*, 1991; Rontoyianni & Mavridis, 1994; Makedonopoulou & Mavridis, 2000), MF forms a monomeric complex with β-CD (Fig. 4). Like most of the known β-CD monomeric inclusion complexes, the MF inclusion complex adopts a herringbone-type packing scheme (Saenger & Steiner, 1998; Mentzafos *et al.*, 1991) in which CD faces are blocked by adjacent CD molecules. The packing is stabilized by guest–host hydrogen bonding (Table 3) and (O···O) intermolecular β-CD—β-CD close contacts (Table 5).

5. Conclusions

The high-resolution powder-diffraction technique, which uses the high intensity of a synchrotron source in combination with molecular simulations, enabled the structure determination of a CD inclusion complex from powder-diffraction data alone. The results show the importance of using different complementary techniques, in particular the important role of the genetic-algorithm search procedure with torsion-angle variation to obtain accurate starting models for RR and the addition of stereochemical restraints in the refinement process.

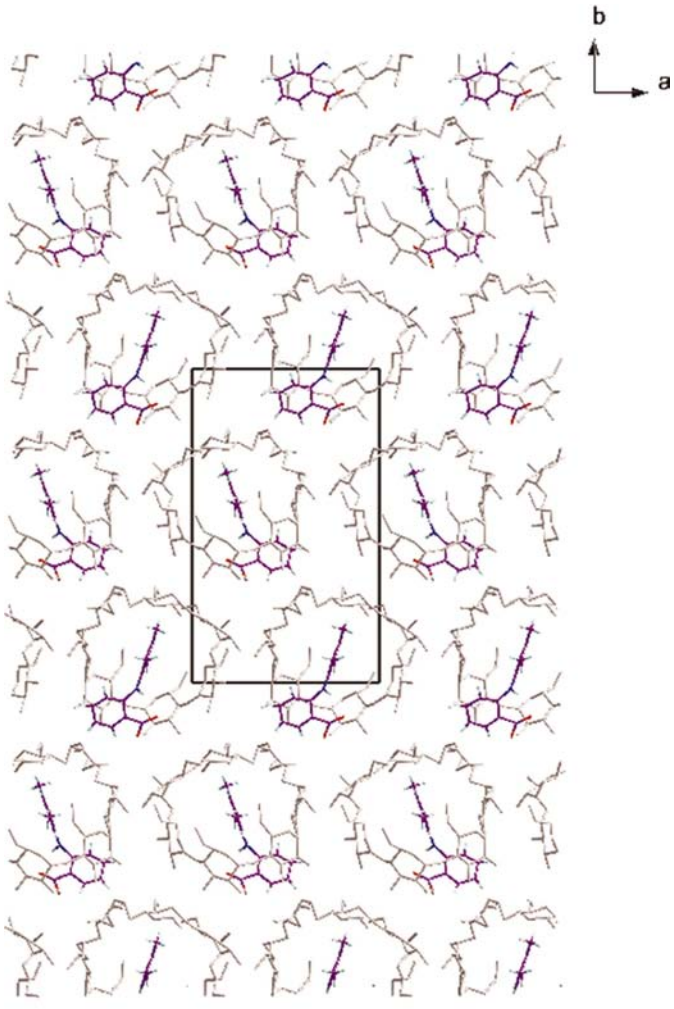

Figure 4
Packing view of (I) along the *c* axis.

Two different inclusion models were found, which corroborate the occurrence of bimodality in this type of CD inclusion compound. The crystal structure that is more likely to be formed in the solid state is suggested by RR.

The authors would like to thank Dr A. N. Fitch from BM16 at the European Synchrotron Radiation Facility for his help during the high-resolution powder-diffraction measurements.

Table 5
Close intermolecular O···O contacts between CDs.

D	*A*	*D*···*A* (Å)
(I)		
O2(G1)	O6(G2)^{i}	2.44 (6)
O6(G3)	O6(G6)^{ii}	2.67 (5)
O3(G5)	O5(G7)$_{iii}$	2.28 (3)
(II)		
O6(G1)	O2(G5)^{iv}	2.79 (6)
O2(G2)	O4(G7)^{ii}	2.53 (3)
O3(G5)	O5(G7)^{iii}	2.72 (3)

Symmetry codes: (i) $x, y, -1+z$; (ii) $-1+x, y, z$; (iii) $1-x, -\frac{1}{2}+y, 1-z$; (iv) $1-x, \frac{1}{2}+y, 1-z$.

References

Allen, F. H. & Kennard, O. (1993). *Chem. Des. Autom. News*, **8**, 31–37.
Ammar, H. O., El-Nahhas, S. A. & Emara, L. H. (1997). *Pharmazie*, **52**, 376–379.
Atwood, J. L., Davies, J. E. D., MacNicol, D. D. & Vogtle, F. (1996). *Comprehensive Supramolecular Chemistry*, Vol. 3, pp. 253–278. UK: Pergamon.
Betzel, C., Saenger, W., Hingerty, B. E. & Brown, G. M. (1984). *J. Am. Chem. Soc.* **106**, 7545–7557.
Caira, M. R. (2003). *Rev. Roum. Chim.* In the press.
Caira, M. R., Griffith, V. J., Nassimbeni, L. R. & VanOudtshoon, B. (1994). *J. Chem. Soc. Chem. Commun.* pp. 1061–1062.
Chernyshev, V. V. & Schenk, H. (1998). *Z. Kristallogr.* **213**, 1–3.
D'Souza, V. T. & Lipkowitz, K. B. (1998). *Chem. Rev.* **98**, 1741–1742.
Fathallah, M., Fotiadu, F. & Jaime, C. (1994). *J. Org. Chem.* **59**, 1288–1293.
Fitch, A. N. (1996). *Materials Science Forum*, Vol. 228, edited by R. J. Cernik, R. Delhez & E. J. Mittemeijer, pp. 219–222.
Fromming, K. H. & Szejtli, J. (1994). *Cyclodextrins in Pharmacy*. Dordrecht: Kluwer Academic.
Fronza, G., Mele, A., Redenti, E. & Ventura, P. (1992). *J. Pharm. Sci.* **81**, 1162–1165.
Hladon, T., Pawlaczyk, J. & Szafran, B. (1999). *J. Incl. Phenom. Macrocyclic Chem.* **35**, 497–506.
Howard, C. J. (1982). *J. Appl. Cryst.* **15**, 615–620.
Irie, T. & Uekama, K. (1997). *J. Pharm. Sci.* **86**, 147–162.
Kostkowski, W. & Kubikowski, P. (1994). *Farmakologia.* Warszawa: PZWL.
Larson, A. C. & Von Dreele, R. B. (1994). *General Structure Analysis System* (*GSAS*). Los Alamos National Laboratory Report LAUR 86–748. Los Alamos National Laboratory, Los Alamos, NV, USA.
Loftsson, T., Baldvinsdottir, J. & Sigurdardottir, A. M. (1993). *Int. J. Pharm.* **98**, 225–230.
Loftsson, T. & Brewster, M. E. (1996). *J. Pharm. Sci.* **85**, 1017–1025.
Loftsson, T., Olafsdottir, B. J., Fridrikdottir, H. & Jonsdottir, S. (1993). *Eur. J. Pharm. Sci.* **1**, 95–101.
Loftsson, T. & Petersen, D. S. (1997). *Pharmazie*, **52**, 783–785.
McConnell, J. F. & Company, F. Z. (1976). *Cryst. Struct. Commun.* **5**, 861–864.
Makedonopoulou, S. & Mavridis, I. M. (2000). *Acta Cryst.* B**56**, 322–331.
Makedonopoulou, S., Tulinski, A. & Mavridis, I. M. (1999). *Supramol. Chem.* **11**, 73–81.
Makedonopoulou, S., Yannakopoulou, K., Mentzafos, D., Lamzin, V., Popov, A. & Mavridis, I. M. (2001). *Acta Cryst.* B**57**, 399–409.
Mentzafos, D., Mavridis, I. M., Le Bas, G. & Tsoucaris, G. (1991). *Acta Cryst.* B**47**, 746–757.
Molecular Simulations Inc. (1995). *Cerius.* Release 2.0. Biosym/Molecular Simulation Inc., San Diego, USA.
Moss, G. P. (1996). *Pure Appl. Chem.* **68**, 2193–2222.
Nogrady, T. (1988). *Medicinal Chemistry*, 2nd ed. Oxford University Press.
Palmieri, G. F., Galli-Angeli, D., Giovannucci, G. & Martelli, S. (1997). *Drug Dev. Ind. Pharm.* **23**, 27–37.
Pennington, W. T. (1999). *J. Appl. Cryst.* **32**, 1028–1029.
Philips Electronics NV (1996). *PROFIT* Version 1.0*c*. Philips Electronic NV, The Netherlands.
Rajewski, R. A. & Stella, V. J. (1996). *J. Pharm. Sci.* **85**, 1142–1169.
Rontoyianni, A. & Mavridis, I. M. (1994). *J. Incl. Phenom. Mol. Recogn. Chem.* **18**, 211–227.

Rontoyianni, A., Mavridis, I. M., Israel, R. & Beurskens, G. (1998). *J. Incl. Phenom.* **32**, 415–428.
Saenger, W. & Steiner, T. (1998). *Acta Cryst.* A**54**, 798–805.
Salvatierra, D., Jaime, C., Virgili, A. & Sanchez-Ferrando, F. (1996). *J. Org. Chem.* **61**, 9578–9581.
Spek, A. L. (1990). *Acta Cryst.* A**46**, C-34.
Steiner, T. & Koellner, G. (1994). *J. Am. Chem. Soc.* **116**, 5122–5128.
Toraya, H. (1986). *J. Appl. Cryst.* **19**, 440–447.
Visser, J. W. (1969). *J. Appl. Cryst.* **2**, 89–95.
Von Dreele, R. B. (1997). *J. Appl. Cryst.* **30**, 517–525.
Zlokazov, V. B. & Chernyshev, V. V. (1992). *J. Appl. Cryst.* **25**, 447–451.